

 Very Important Paper

Phosphonate as a Stable Zinc-Binding Group for “Pathoblocker” Inhibitors of Clostridial Collagenase H (ColH)

Katrin Voos,^[a] Esther Schönauer,^[b] Alaa Alhayek,^[c, e] Jörg Haupenthal,^[c] Anastasia Andreas,^[d, e] Rolf Müller,^[d, e] Rolf W. Hartmann,^[c, e] Hans Brandstetter,^[b] Anna K. H. Hirsch,^{*[c, e]} and Christian Ducho^{*[a]}

Microbial infections are a significant threat to public health, and resistance is on the rise, so new antibiotics with novel modes of action are urgently needed. The extracellular zinc metalloprotease collagenase H (ColH) from *Clostridium histolyticum* is a virulence factor that catalyses tissue damage, leading to improved host invasion and colonisation. Besides the major role of ColH in pathogenicity, its extracellular localisation makes it a highly attractive target for the development of new antivirulence agents. Previously, we had found that a highly selective and potent thiol produg (with a hydrolytically cleavable

thiocarbamate unit) provided efficient ColH inhibition. We now report the synthesis and biological evaluation of a range of zinc-binding group (ZBG) variants of this thiol-derived inhibitor, with the mercapto unit being replaced by other zinc ligands. Among these, an analogue with a phosphonate motif as ZBG showed promising activity against ColH, an improved selectivity profile, and significantly higher stability than the thiol reference compound, thus making it an attractive candidate for future drug development.

Introduction

Due to emerging resistances against established antibacterial agents, the treatment of bacterial infections might be thrown back to a state similar to the pre-antibiotic era. In an estimated

worst-case scenario, it has been predicted that by 2050, infectious diseases caused by antibiotic-resistant microbes might lead to higher death tolls than cancer does today.^[1] Hence, there is an urgent need to develop antibiotics with novel modes of action, high efficacy and a reduced tendency to induce the development of resistances.^[2]

A promising way of overcoming the problem of fast resistance development is the design of so-called “pathoblockers”, that is, compounds that target virulence factors rather than vital factors of bacteria, in contrast to classical antibiotics.^[3] Bacteria that are thus “disarmed” by pathoblockers should ideally cause either no or at least a strongly attenuated disease. Furthermore, such pathoblocker-induced reduction of pathogenicity should provide the immune system the necessary time to develop a full humoral and cellular immune response to eliminate the bacteria, possibly aided by a low-dose adjunctive treatment with antibiotics.

Clostridium (including the prominent species *C. difficile*, *C. histolyticum* (*Hathewayia histolytica*), *C. tetani*, *C. botulinum*, *C. septicum*, and *C. perfringens*) is a genus of Gram-positive anaerobic bacteria that is ubiquitous. They cause severe human diseases such as tetanus, gas gangrene (myonecrosis), botulism, bacterial corneal keratitis, and other dangerous infections^[4] with high mortality rates.^[5] Some of these species have even been cultivated and are bioweapons.^[6]

Collagenase is a prominent virulence factor for the progression of Clostridia-associated diseases.^[7] It is a calcium- and zinc-dependent metalloprotease that destroys the host’s connective tissue and uses it as a carbon source. This leads to improved host invasion and colonisation and hence to breaching of the human immune system. Also, the spread of toxins into the damaged tissue is promoted.^[5b,8] Collagens, the natural


[a] K. Voos, Prof. Dr. C. Ducho
 Department of Pharmacy, Pharmaceutical and Medicinal Chemistry
 Saarland University
 Campus C2 3, 66123 Saarbrücken (Germany)
 E-mail: christian.ducho@uni-saarland.de


[b] Dr. E. Schönauer, Prof. Dr. H. Brandstetter
 Department of Biosciences and
 Christian Doppler Laboratory for Innovative Tools for Biosimilar Characterization
 Division of Structural Biology, University of Salzburg
 Billrothstrasse 11, 5020 Salzburg (Austria)

[c] A. Alhayek, Dr. J. Haupenthal, Prof. Dr. R. W. Hartmann,
 Prof. Dr. A. K. H. Hirsch
 Department of Drug Design and Optimization
 Helmholtz Institute for Pharmaceutical Research Saarland (HIPS)
 Helmholtz Centre for Infection Research (HZI)
 Campus E8 1, 66123 Saarbrücken (Germany)
 E-mail: anna.hirsch@helmholtz-hips.de

[d] A. Andreas, Prof. Dr. R. Müller
 Department of Microbial Natural Products
 Helmholtz Institute for Pharmaceutical Research Saarland (HIPS)
 Helmholtz Centre for Infection Research (HZI)
 Campus E8 1, 66123 Saarbrücken (Germany)

[e] A. Alhayek, A. Andreas, Prof. Dr. R. Müller, Prof. Dr. R. W. Hartmann,
 Prof. Dr. A. K. H. Hirsch
 Department of Pharmacy, Saarland University
 Campus E8 1, 66123 Saarbrücken (Germany)

 Supporting information for this article is available on the WWW under <https://doi.org/10.1002/cmdc.202000994>

 © 2021 The Authors. ChemMedChem published by Wiley-VCH GmbH. This is an open access article under the terms of the Creative Commons Attribution License, which permits use, distribution and reproduction in any medium, provided the original work is properly cited.

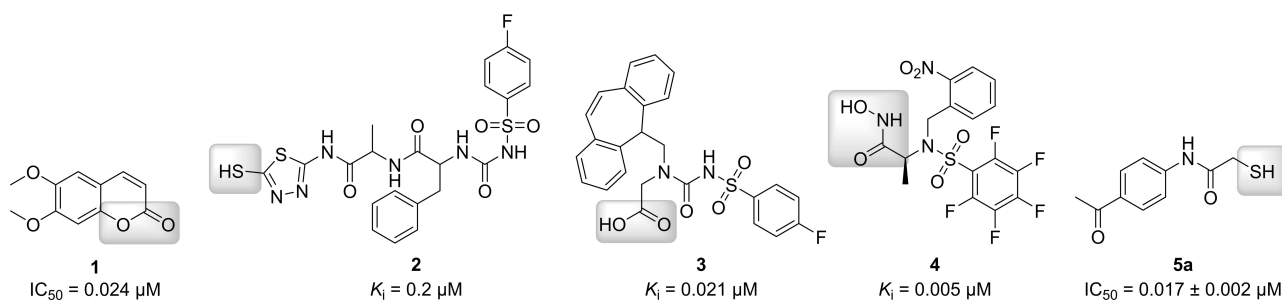


Figure 1. Structural diversity of selected previously reported ColH inhibitors with the zinc-binding groups highlighted in grey.^[9]

substrates of ColH, are the most abundant proteins of the human extracellular matrix and can be found throughout all organs (especially in skin, bones and joints). Their triple-helical structure is formed by three intertwined left-handed helices and is based on a shared repetitive Gly- X_{aa} - Y_{aa} motif. In this motif, X_{aa} and Y_{aa} can be nearly any amino acid, but a proline in the X_{aa} (28%) and a hydroxyproline in the Y_{aa} (38%) position, respectively, occur most frequently.^[10]

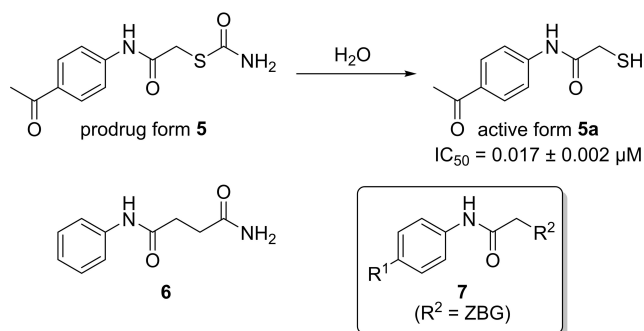
Clostridial collagenases are multidomain proteins whose collagenolytic core is composed of an activator domain and a peptidase domain.^[11] In the latter, the catalytic zinc ion is coordinated by two histidines in an HEXXH motif and a downstream glutamate.^[5a,11] Mechanistically, the general acid-base glutamate in the HEXXH motif polarises the nucleophilic water molecule in the active site. This polarisation is further facilitated by the zinc ion acting as a Lewis acid (promoted water mechanism). Additionally, by polarising and stabilising the carbonyl oxygen, the zinc ion simultaneously increases the electrophilicity of the carbonyl carbon atom of the scissile amide bond in the bound collagen substrate.^[12] Co-crystal structures of collagenase H (ColH) and collagenase G (ColG) from *C. histolyticum* with a selective and an unselective binder, respectively, are available (PDB IDs: ColH with selective inhibitor: 5O7E,^[13] ColG with unselective inhibitor: 2Y6I^[11]). Clostridial collagenases represent “true” collagenases, that is, they are collagen-specific and can degrade collagen in its native triple-helical structure. This cleavage can occur at multiple sites, thus generating small peptide fragments.^[7,8a] In contrast, human matrix metalloproteases (MMPs), that also include “true” collagenases, are only able to cleave collagen at one site.^[14] After cleavage, the collagen fragments then have to undergo further hydrolytic steps catalysed by different enzymes.

Besides the crucial role of clostridial collagenases in disease development, their extracellular localisation^[7] makes them highly attractive drug targets. The penetration of the bacterial cell wall often represents a major challenge for antibacterial drug development,^[15] but can thus be avoided in this case. Naturally occurring collagenase-inhibiting coumarin derivatives (e.g., 1, Figure 1) were found in extracts of *Viola yedoensis*.^[9a] Supuran and co-workers have made major contributions to the emerging field of synthetic inhibitors of bacterial collagenases. They have prepared and studied a variety of compounds that mimic the natural substrate with an amide backbone and bind

strongly to the active site via a zinc-binding group (ZBG). The latter coordinates to the zinc ion and displaces the essential water molecule from the active site. The inhibitors vary in their different ZBG, including 2-mercapto-substituted 1,3,4-thiadiazole (e.g., 2),^[9b] carboxylate (e.g., 3),^[9c] and hydroxamic acid units (e.g., 4;^[9d-f] Figure 1). However, all of these compounds show one major drawback in that they are also strong inhibitors of human MMPs due to highly homologous motifs in the active sites of both enzyme families. These off-target effects severely limit their potential to become suitable drug candidates.

More recently, we have reported the first selective inhibitor 5 of bacterial collagenases. “Hit” compound 5 contains a thiocarbamate unit as a hydrolytically cleavable prodrug moiety of the thiol 5a, which then strongly binds to the zinc ion and therefore inhibits ColH in the low-nanomolar range (Scheme 1).^[13] This compound was also co-crystallised with the target enzyme, revealing the exact binding mode in the non-primed binding region. The interactions with the non-primed edge strand, whose conformation is conserved and distinct for clostridial collagenases, provide the high selectivity towards various bacterial collagenases, including ColH and ColG from *C. histolyticum*, ColT from *C. tetani*, and ColQ1 from *Bacillus cereus*, over the unwanted inhibition of human MMPs.^[13]

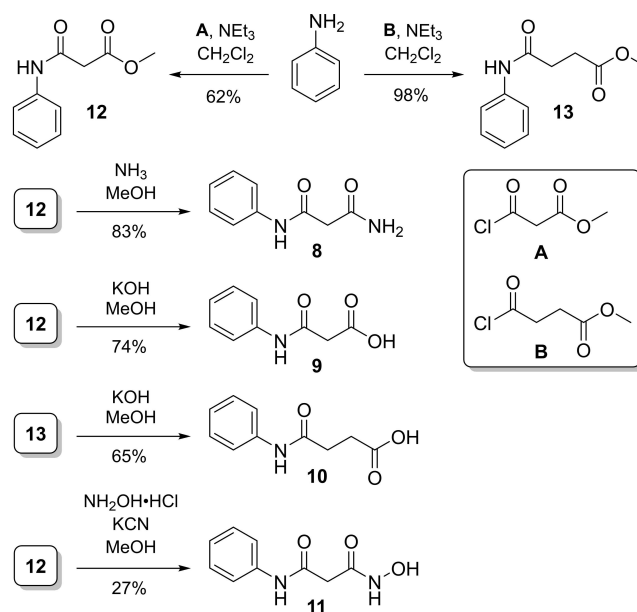
Very recently, we demonstrated that the linker unit in structures of type 5a, that is, the motif connecting the aromatic moiety and the thiol ZBG, can be varied. Thus, cyclisation to a



Scheme 1. Structures of the previously identified “hit” ColH inhibitor 5, its active thiol form 5a (after prodrug cleavage) and previously reported amide analogue 6. General structure 7 of the novel potential collagenase inhibitors reported in this work (ZBG = zinc-binding group).

succinimide is tolerated with a moderate loss of activity if the thiol is kept in its relative position.^[16] This, however, indicated that inhibitor **5a** can be further varied and optimised. One obvious objective of such an optimisation process would be the replacement of the ZBG. Even though there are thiol-containing drugs in clinical use,^[17a,b] thiols generally suffer from their limited stability, mainly due to oxidative disulfide formation that often leads to rapid inactivation.^[17c] Therefore, a replacement of the thiol with a different ZBG would be highly useful, even if it might potentially lead to some loss of inhibitory activity. Our goal was to retain the high selectivity of **5a** for the inhibition of bacterial collagenases vs. human off-targets. Hence, the *N*-arylacamide core structure was kept intact and only the thiol moiety as the metal-binding group was exchanged for various other ZBGs. Among the significant number of zinc-binding units described in the literature,^[18] we decided to focus on sterically smaller motifs in order to retain the previously identified binding mode.^[13]

An amide **6** as a stable analogue of the thiocarbamate structure of prodrug **5** (Scheme 1) has already been reported by us.^[13] Amide **6** had the same length as the thiocarbamate **5**. However, it was more than 400-fold less potent as a ColH inhibitor. This result suggested to us that the overall length of **6** might not fit into the ColH active site, as the (shorter) thiol **5a** (and not thiocarbamate **5**) was the actual zinc-binding inhibitor. This consideration has significantly influenced our design of the novel series **7** of potential ColH inhibitors described herein (Scheme 1). Thus, most of the new target compounds contained only one methylene unit to connect the amide carbonyl of the core structure and the ZBG (in analogy to **5a**). In this work, we therefore report the synthesis and biological evaluation of 16 novel analogues of **5a** with alternative, more stable ZBGs attached to the core structure (general structure **7**, Scheme 1).



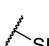
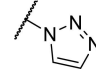
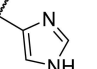
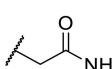
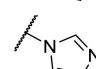
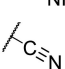
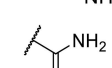
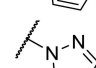
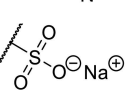
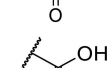
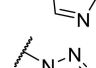
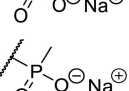
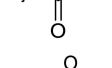
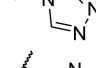
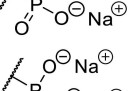
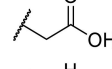
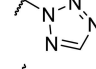
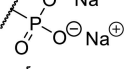
Scheme 2. Synthesis of target compounds **8–11**.

Results and Discussion

Chemistry

As a first set of target compounds, we prepared new analogues **8–11** with amide (**8**), carboxylate (**9**, **10**) and hydroxamate (**11**) units as potential ZBG (Scheme 2, see also Table 1). Succinic acid derivative **10** is a notable exception to the aforementioned design principle (cf. general structure **7**; Scheme 1) as it was the higher homologue of malonic acid derivative **9** and the acid

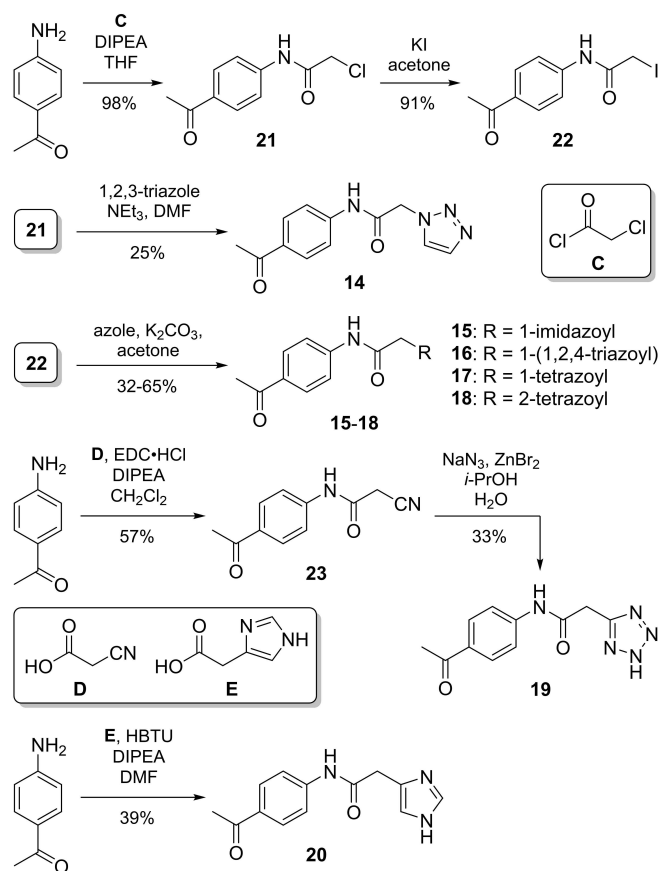
Table 1. *In vitro* inhibitory activities of all synthesised target compounds as well as reference compounds **5a** and **6** against ColH.

Cpd.	R ¹	R ²	IC ₅₀ [μM]	Cpd.	R ¹	R ²	IC ₅₀ [μM]	Cpd.	R ¹	R ²	IC ₅₀ [μM]
5a	Ac		0.017 ± 0.002 ^[13]	14	Ac		> 500	20	Ac		> 500
6	H		> 500 ^[13]	15	Ac		448 ± 33	23	Ac		> 500
8	H		> 500	16	Ac		> 500	24	Ac		> 500
9	H		> 500	17	Ac		> 500	25	Ac		> 500
10	H		> 500	18	Ac		> 500	26	Ac		7 ± 1
11	H		~500	19	Ac		22 ± 1	27	Ac		> 500

derivative of amide **6**, thus having one extra methylene unit to connect the ZBG to the core structure.

Target compounds **8–11** were obtained via acylation of aniline to give methyl esters **12** and **13** as intermediates in 62 and 98% yield, respectively. Subsequently, **12** was treated with ammonia, potassium hydroxide or hydroxylamine to furnish **8**, **9** and **11**, respectively, in 27 to 83% yield. Ester saponification of **13** afforded **10** in 65% yield (Scheme 2).

The zinc ion in the active site of ColH is complexed by two histidine residues.^[5a,11,13] Therefore,azole compounds **14–20** (Scheme 3, see also Table 1) were synthesised to mimic the imidazole moiety of histidine. Triazole derivative **14** was prepared in the following manner. Acylation of *p*-aminoacetophenone with chloroacetyl chloride gave alkyl chloride **21** in 98% yield, and alkylation of 1,2,3-triazole with **21** furnished **14** in 25% yield. In order to obtain an alkylating agent with higher reactivity, **21** was converted into alkyl iodide **22** in a Finkelstein reaction (91% yield). Iodide **22** was then used for the alkylation of other azoles, affording target compounds **15–18** in 32–65% yield. Amide coupling of *p*-aminoacetophenone and cyanoacetic acid gave nitrile intermediate **23** in 57% yield, which was transformed into the target tetrazole **19** by zinc-catalysed cycloaddition with sodium azide (33% yield). Imidazole-derived analogue **20** was synthesised in one step (by amide coupling of *p*-aminoacetophenone) in 39% yield (Scheme 3).



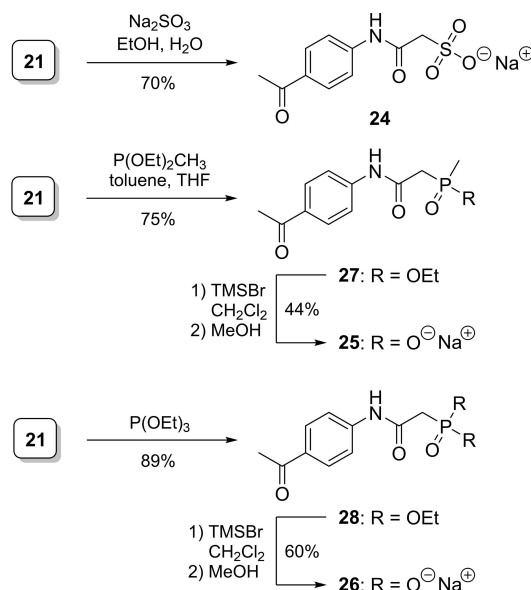
Scheme 3. Synthesis ofazole-derived target compounds **14–20**.

In order to exploit the potential of electrostatic interactions, negatively charged ZBGs were also explored. Hence, target compounds **24** (with a sulfonate unit as ZBG), **25** (phosphinate), and **26** (phosphonate) were synthesised using the previously employed alkyl chloride intermediate **21** (Scheme 4). Sulfonate **24** was obtained by alkylation of sulfite in 70% yield. Both phosphinate **25** and phosphonate **26** were prepared in two steps each, with the first step being a Michaelis–Arbuzov reaction to give ethyl esters **27** and **28** in 75 and 89% yield, respectively. This was followed by silyl-mediated cleavage of the ethyl ester to afford (after ion exchange) highly pure sodium salts **25** and **26** in yields of 44 and 60%, respectively.

In vitro inhibition of ColH

All synthesised target compounds were tested in a previously described FRET-based *in vitro* assay for ColH inhibition, using a custom-made quenched fluorescent peptide as substrate.^[13] The inhibitory activities (IC_{50} values) were obtained from steady-state kinetics. Varying concentrations of the compounds were preincubated with the peptidase domain of ColH (10 nM) for 1 h before the reactions were started by the addition of the peptide substrate. IC_{50} values were determined by nonlinear regression analysis and are listed in Table 1.

Interestingly, only two out of the 16 tested compounds with various zinc-binding groups showed notable inhibitory activity against ColH. These were tetrazole derivative **19** (IC_{50} = 22 μ M) and phosphonate **26** (IC_{50} = 7 μ M). However, both compounds were considerably weaker inhibitors of ColH than thiol **5a** (IC_{50} = 17 nM). As **26** was about three times more active than **19**, it was decided to further investigate phosphonate **26** for other biological properties in order to elucidate if it might be a suitable alternative to **5a**, in spite of its decreased inhibitory potency towards the target collagenase ColH.



Scheme 4. Synthesis of anionic target compounds **24–26**.

Selectivity over potential human off-targets

Inhibitors of bacterial collagenases might potentially also bind to human zinc-dependent enzymes as “off-targets”, even though the results obtained with thiocarbamate **5** had demonstrated that pronounced selectivity can be achieved (see above).^[13] We have therefore investigated if phosphonate **26** (in comparison to thiol **5a** as the active form of **5**) inhibited a selection of such zinc-dependent human off-targets. Our goal was to at least retain the selectivity of “hit” compound **5** when the ZBG is changed. The human enzymes chosen for this study were six representatives of the MMP family, histone deacetylases 3 (HDAC-3) and 8 (HDAC-8), and the tumour necrosis factor α (TNF- α) converting enzyme (TACE, also known as ADAM-17). It should be noted that **5** had previously only been tested for the unwanted inhibition of MMPs.^[13]

Inhibitory activities of both **5a** and novel ColH inhibitor **26** against this panel of potential human off-targets are provided in Table 2 (as percentage inhibition at a fixed concentration of 100 μM). Against the six selected MMP enzymes, both ColH inhibitors showed no notable to very moderate inhibition at this rather high concentration. An exception was the inhibition of MMP-8 (36% @100 μM) and MMP-14 (47% @100 μM), respectively, by phosphonate **26**. In contrast, both enzymes were not inhibited by thiol **5a**.^[13] However, this implies that the *in vitro* inhibitory activities of **26** towards these two representatives of the MMP family were still more than one order of magnitude lower than towards ColH as its bacterial target. Overall, the rather limited inhibition of MMPs as human off-targets by **26** confirmed our initial design principle to retain the aromatic anilide core structure that had been shown to be crucial for the selectivity of **5/5a**.^[13]

As noted, the other potential human off-targets investigated in this context were two representatives of the HDAC family and TACE. Regarding the unwanted inhibition of these three enzymes, phosphonate **26** was superior to thiol **5a** throughout (Table 2). Thus, thiol **5a** showed significantly higher inhibition of the two HDAC tested (~50% inhibition with **5a** vs. maximum ~10% with **26**) and in particular of TACE (~80% with **5a** vs. ~20% with **26**). The unwanted inhibition of TACE would lead to a decreased release of TNF- α , hence causing a reduced immune

response of the host^[19] and thereby providing the bacteria with a higher chance to establish a critical infection.^[20] The absence of notable HDAC and TACE inhibition for **26** represents a major advantage of this novel phosphonate-derived ColH inhibitor.

Cytotoxicity against human cells

The new ColH inhibitor **26** was also investigated for potential cytotoxic effects against three representative human cell lines, that is, HepG2, HEK293, and A549 cells. Within the experimental error, **26** showed a comparable or even slightly lower decrease of cell viability (as an indicator of toxicity) than the previous “hit” compound **5a** in all investigated cell lines at 100 μM compound concentration (Table 3). As a reference compound, the approved antibiotic rifampicin (that is clinically used in the long-term therapy of tuberculosis^[21]) was also studied. Rifampicin showed a comparable decrease of cell viability as both tested ColH inhibitors **26** and **5a** at an identical concentration (100 μM). As further references and also as positive controls, the chemotherapeutic agents doxorubicin^[22a] and epirubicin^[22b] were employed and were found to be notably toxic at a 100-fold lower concentration (i.e., 1 μM) in all three cell lines. In turn, it can be concluded that even a 100-fold higher concentration of **26** might be tolerated based on these cytotoxicity studies.

Toxicity in a zebrafish model

In order to determine the toxicity of ColH inhibitors **26** and **5a** in an *in vivo* setting, a zebrafish larvae toxicity assay was performed. Zebrafish are very small and almost transparent organisms. They can be cultured in small volumes of media, leading to very small amounts of compounds being needed for testing. Furthermore, zebrafish develop their organ systems, which show high similarity to the mammalian cardiovascular, nervous, and digestive systems,^[23a,b] in less than one week,^[23a,c,d] thus making the experiments fast and relatively inexpensive. Using this assay, we aimed to determine the maximally tolerated dose (MTD) at which no toxic effects of the compounds were observed. It was found that both phosphonate **26** and thiol reference **5a** showed no toxic effects at concentrations up to 100 μM .

Table 2. *In vitro* inhibitory activities of novel ColH inhibitor **26** (ZBG = phosphonate) and reference compound **5a** (ZBG = thiol) against a panel of potential human off-targets.

Human enzyme	Inhibition [%] at 100 μM compound ^[a]	
	5a (thiol)	26 (phosphonate)
MMP-1	n.i. ^[b]	19 \pm 4
MMP-2	19 \pm 8	18 \pm 1
MMP-3	n.i.	n.i.
MMP-7	n.i.	n.i.
MMP-8	n.i.	36 \pm 1
MMP-14	n.i.	47 \pm 13
HDAC-3	51 \pm 7	11 \pm 2
HDAC-8	48 \pm 5	n.i.
TACE	79 \pm 7	21 \pm 8

[a] Means of at least two independent measurements, 10 nM enzyme concentration. [b] n.i. = no inhibition (< 10%).

Table 3. Cytotoxicity (as decrease of cell viability) of ColH inhibitors **26** (ZBG = phosphonate) and **5a** (ZBG = thiol) as well as of three reference compounds against three human cell lines.

Compound	c [μM]	Decrease of viability [%] after 48 h ^[a]		
		HepG2	HEK293	A549
5a (thiol)	100	15 \pm 9	53 \pm 0	18 \pm 12
26 (phosphonate)	100	8 \pm 10	32 \pm 4	20 \pm 2
rifampicin	100	33 \pm 13	29 \pm 13	9 \pm 13
doxorubicin	1	57 \pm 14	47 \pm 9	53 \pm 13
epirubicin	1	68 \pm 10	49 \pm 11	56 \pm 12

[a] Means of at least two independent measurements.

Ex vivo pig skin degradation assay

To investigate the activity of collagenase inhibitors on tissue in a more complex experimental setting, an *ex vivo* pig skin degradation assay using purified ColQ1 from *B. cereus* has recently been developed.^[16] The degradation of collagen in this mammalian tissue was measured as a rate of hydroxyproline (Hyp) release. This assay had previously been used to demonstrate the efficacy of succinimide **29** (Figure 2) as an inhibitor of bacterial collagenase activity.^[16] Succinimide derivative **29** had an IC_{50} value of $0.06 \pm 0.01 \mu\text{M}$ against ColH *in vitro*, which indicates that it is ca. 100-fold more potent than phosphonate **26**. Towards ColQ1 (at a fixed inhibitor concentration of $100 \mu\text{M}$), **29** had shown complete ($100 \pm 2\%$) inhibition, which corresponded to an IC_{50} value significantly below $100 \mu\text{M}$.^[16] Using the same *in vitro* assay, novel phosphonate **26** had an IC_{50} value of $183 \pm 7 \mu\text{M}$. However, in the *ex vivo* assay, **26** reduced the formation of Hyp to 75% of the Hyp production of the control at a concentration of $100 \mu\text{M}$, which is nearly identical to the potency of **29** (Figure 3).

Overall, succinimide **29** showed a stronger reduction of Hyp formation at elevated concentrations than phosphonate **26**, in particular at 300 and $400 \mu\text{M}$, respectively (Figure 3). However, this difference in potency was far less than what was expected based on the significant difference of the aforementioned *in vitro* activities (IC_{50} values). It should also be noted that succinimide **29** appears to reach a “plateau” in activity between about 300 and $400 \mu\text{M}$ while phosphonate **26** had a nearly linear correlation of concentration and activity. This “plateau” in the activity of **29** might eventually result from disulfide

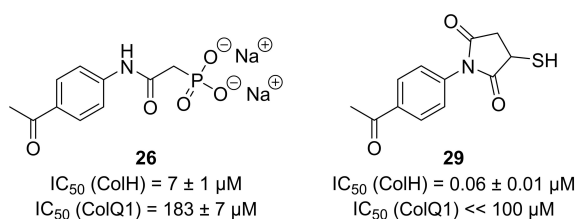


Figure 2. Structures and *in vitro* potencies for collagenase inhibition of compounds **26** and **29**.^[16]

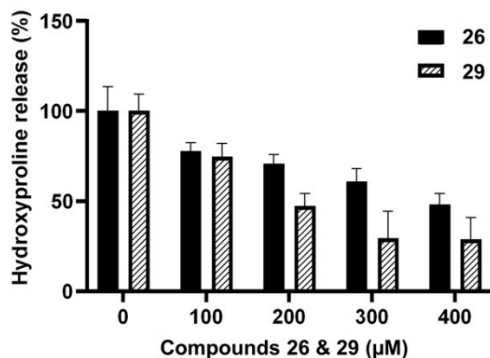


Figure 3. *Ex vivo* pig skin degradation assay: hydroxyproline release after 24 h upon treatment with **26** and **29**^[16] (in % relative to the controls).

formation at higher concentrations. This again highlights the benefit of employing an oxidation-resistant ZBG (as in **26**) to provide air-stable alternatives to thiol-derived inhibitors.

Conclusions

In summary, we herein report the exchange of the thiol ZBG of previously published selective ColH inhibitors with more stable ZBGs, with the selectivity of the thiol-based “hit” compound **5a** being retained. Thus, the structure of **5a** was varied to furnish phosphonate derivative **26**. In contrast to the thiol group in **5a**, the phosphonate as a ZBG in **26** is not prone to oxidation or degradation. Novel inhibitor **26** still showed reasonably potent (i.e., micromolar) inhibition of the clostridial collagenase ColH, while apparently retaining the binding mode of **5a** and therefore its remarkable selectivity over potential human off-targets such as MMPs. In comparison to **5a**, we observed a better selectivity of **26** over other human off-targets (HDAC and TACE), suggesting it might be an improved hit structure for further development. Inhibitor **26** showed no indication of major toxicity in three different human cell lines as well as high tolerance in an *in vivo* zebrafish toxicity assay. Furthermore, we demonstrated the efficacy of **26** not only in an *in vitro* enzyme assay for collagenase activity, but also in a more complex *ex vivo* pig skin degradation assay. The results from this assay highlight the potency of **26** and the relevance of a stable (non-thiol) ZBG for biological activity in a complex biological setting. Overall, **26** should therefore be considered as a new improved hit structure for the development of potent inhibitors of bacterial collagenases that will now undergo further optimisation in our laboratories.

Experimental Section

General methods: All chemicals, starting materials and reagents were purchased from standard suppliers and used without further purification. Air- and/or water-sensitive reactions were carried out under nitrogen atmosphere with anhydrous solvents. Anhydrous solvents were obtained in the following manner: THF, DMF and CH_2Cl_2 were dried with a solvent purification system (MBRAUN MB SPS 800). All other solvents were of technical quality and distilled prior to use, and deionised water was used throughout. Reactions were monitored by TLC on aluminium plates precoated with silica gel 60 F254 (VWR). Visualisation of the spots was carried out using UV light (254 nm) and/or staining under heating (VSS stain: 4 g vanillin, 25 mL conc. H_2SO_4 , 80 mL AcOH, 680 mL MeOH; CAM stain: 12 g ammonium molybdate, 0.5 g ceric ammonium molybdate, 235 mL H_2O , 15 mL conc. H_2SO_4 ; ninhydrin stain: 1.5 g ninhydrin, 100 mL *n*-butanol, 3.0 mL AcOH). R_f values are given to the nearest 0.05. Column chromatography was carried out on silica gel 60 (40–63 μm , 230–400 mesh ASTM, VWR) under flash conditions. Preparative centrifugal TLC was performed on a Chromatotron™ 7924T (T-Squared Technology) using glass plates coated with silica gel 60 PF₂₅₄ containing a fluorescent indicator (VWR, thickness depending on the amount of crude material to be separated, for 50–500 mg: 1 mm layer). Ion-exchange chromatography was carried out using DOWEX™ 50WX8 resin (200–400 mesh, VWR) in the Na^+ form. Semipreparative HPLC was performed on a VWR-Hitachi system equipped with an L-2300 pump, an L-2200 autosampler, an L-2455

diode array detector (DAD) and a LichroCart™ Purospher™ RP18e column (5 μm, 10×250 mm, VWR). NMR spectra were recorded using the following Bruker NMR spectrometers: for ¹H NMR spectra at 500 MHz and ¹³C NMR spectra at 126 MHz: Avance™ 500; for ³¹P NMR spectra at 203 MHz: Avance™ 500. For the assignment of signals, ¹H,¹H COSY, ¹H,¹³C HSQC and ¹H,¹³C HMBC spectra were used. All ¹³C and ³¹P NMR spectra are ¹H-decoupled. All spectra were recorded at room temperature if not indicated otherwise and were referenced internally to solvent residual signals wherever possible. Chemical shifts (δ) are quoted in ppm and coupling constants (*J*) are reported in Hz. Low-resolution mass spectra were recorded on a liquid chromatography-coupled mass spectrometer (LC-MS) Surveyor MSQ Plus from Finnigan. For the LC separation prior to detection, a Nucleodur™ 100–5 C₁₈ column (5 μm, 3×125 mm) was used. High-resolution mass spectra were recorded on a Thermo Scientific Q Exactive Orbitrap mass spectrometer with ESI ionisation mode coupled with an Ultimate 3000 HPLC system by Thermo Scientific, equipped with a Thermo Accucore™ phenyl-X column (2.1 μm, 3×100 mm). Melting points (mp) were measured on a melting point apparatus SMP3 (Stuart Scientific) and were not corrected.

General procedure (GP1) for the synthesis of azole derivatives: Alkyl iodide **22** (1.0 equiv), K₂CO₃ (1.1 equiv), and the respective azole (1.1 equiv) were suspended in acetone (20 mL, ~25 mM) and stirred at 70 °C overnight (15–20 h). EtOAc (200 mL) was added, and the organic layer was washed with water (3×30 mL) and brine (50 mL) and dried over Na₂SO₄. The solvent was evaporated under reduced pressure and the resultant crude product was purified by column chromatography to give the respective azole derivative.

General procedure (GP2) for the cleavage of ethyl esters: The respective ethyl ester (1.0 equiv) was dissolved in CH₂Cl₂ (10 mL). TMSBr (5.0 equiv) was added dropwise over 10 min, and the reaction was stirred at RT overnight (15–20 h). MeOH (10 mL) was then added, and the mixture was stirred for 1–2 h. The solvent was evaporated under reduced pressure, the resultant crude product was purified by HPLC and the obtained product was converted into its Na⁺ form by ion-exchange column chromatography to give the respective title compound.

N¹-Phenylmalonamide (8): Methyl ester **12** (49 mg, 0.25 mmol) was dissolved in MeOH (6 mL). NH₃ solution (33%, 3 mL) was added, and the reaction mixture was stirred at RT overnight. The solvent was evaporated under reduced pressure and the resultant crude product was purified by column chromatography (CH₂Cl₂/MeOH 100:0→95:5) to give **8** as a white solid (37 mg, 83%). ¹H NMR (500 MHz, [D₆]DMSO): δ = 10.07 (s, 1H, Ph-NH), 7.58 (d, *J* = 7.6 Hz, 2H, 2'-H, 6'-H), 7.51 (br, 1H, NH₂-a), 7.30 (t, *J* = 7.9 Hz, 2H, 3'-H, 5'-H), 7.11 (br, 1H, NH₂-b), 7.04 (t, *J* = 7.4 Hz, 1H, 4'-H), 3.21 (s, 2H, 2-H) ppm. ¹³C NMR (126 MHz, [D₆]DMSO): δ = 168.68 (C-1 or C-3), 165.74 (C-1 or C-3), 138.96 (C-1'), 128.71 (C-3', C-5'), 123.27 (C-4'), 119.02 (C-2', C-6'), 44.50 (C-2) ppm. HRMS (ESI): calcd. for C₉H₁₁N₂O₂ [M+H]⁺ 179.0815, found 179.0813. TLC (petroleum ether/EtOAc 1:1): R_f = 0.10.

3-Oxo-3-(phenylamino)propanoic acid (9): Methyl ester **12** (102 mg, 0.528 mmol) was dissolved in MeOH (5 mL). KOH solution (50 g/L, 1.2 mL) was added, and the reaction mixture was stirred at 35 °C for 4 h. It was then acidified with HCl, and EtOAc (200 mL) was added. The organic layer was washed with HCl (2 M, 4×40 mL) and brine (50 mL) and then dried over Na₂SO₄. The solvent was evaporated under reduced pressure, and the resultant crude product was purified by column chromatography (CH₂Cl₂/MeOH/HCOOH 95:4:1) to give **9** as a white solid (70 mg, 74%). ¹H NMR (500 MHz, [D₆]DMSO): δ = 12.68 (br, 1H, COOH), 10.13 (s, 1H, NH), 7.57 (d, *J* = 7.6 Hz, 2H, 2'-H, 6'-H), 7.31 (t, *J* = 7.9 Hz, 2H, 3'-H, 5'-H), 7.05 (t, *J* = 7.4 Hz, 1H, 4'-H), 3.34 (s, 2H, 2-H) ppm. ¹³C NMR

(126 MHz, [D₆]DMSO): δ = 169.28 (C-1 or C-3), 164.57 (C-1 or C-3), 138.95 (C-1'), 128.76 (C-3', C-5'), 123.38 (C-4'), 119.01 (C-2', C-6'), 43.99 (C-2) ppm. HRMS (ESI): calcd. for C₉H₁₀NO₃ [M+H]⁺ 180.0655, found 180.0654. TLC (petroleum ether/EtOAc/HCOOH 49:49:2): R_f = 0.20.

4-Oxo-4-(phenylamino)butanoic acid (10): Methyl ester **13** (204 mg, 0.985 mmol) was dissolved in MeOH (4 mL). KOH solution (50 g/L, 2.2 mL) was added, and the reaction mixture was stirred at 35 °C for 4 h. It was then acidified with HCl and EtOAc (200 mL) was added. The organic layer was washed with HCl (2 M, 4×40 mL) and brine (50 mL) and then dried over Na₂SO₄. The solvent was evaporated under reduced pressure, and the resultant crude product was purified by column chromatography (petroleum ether/EtOAc/HCOOH 70:29:1) to give **10** as a white solid (124 mg, 65%). ¹H NMR (500 MHz, [D₆]DMSO): δ = 12.20 (br, 1H, COOH), 9.94 (br, 1H, NH), 7.57 (d, *J* = 7.6 Hz, 2H, 2'-H, 6'-H), 7.28 (t, *J* = 7.9 Hz, 2H, 3'-H, 5'-H), 7.01 (t, *J* = 7.4 Hz, 1H, 4'-H), 2.56–2.50 (m, 4H, 2-H, 3-H) ppm. ¹³C NMR (126 MHz, [D₆]DMSO): δ = 173.83 (C-1 or C-4), 170.06 (C-1 or C-4), 139.30 (C-1'), 128.65 (C-3', C-5'), 122.88 (C-4'), 118.87 (C-2', C-6'), 31.04 (C-2 or C-3), 28.82 (C-2 or C-3) ppm. HRMS (ESI): calcd. for C₁₀H₁₂NO₃ [M+H]⁺ 194.0812, found 194.0810. TLC (petroleum ether/EtOAc/HCOOH 49:49:2): R_f = 0.25.

N¹-Hydroxy-N²-phenylmalonamide (11): Hydroxylamine hydrochloride (497 mg, 7.15 mmol), DIPEA (1.50 mL, 8.61 mmol) and KCN (19 mg, 0.29 mmol) were dissolved in MeOH (5 mL), and the mixture was heated to reflux. After 10 min, a solution of methyl ester **12** (91 mg, 0.47 mmol) in MeOH (5 mL) was added, and the reaction mixture was stirred under reflux overnight. It was then concentrated under reduced pressure, acidified with HCl (1 M, 100 mL) and extracted with EtOAc (5×50 mL). The combined organics were dried over Na₂SO₄, and the solvent was evaporated under reduced pressure. The resultant crude product was purified by HPLC (water+0.1% TFA, MeCN+0.1% TFA, 95:5→0:100) to give **11** as a slightly orange solid (25 mg, 27%). ¹H NMR (500 MHz, [D₆]DMSO): δ = 10.61 (s, 1H, NHOH), 10.10 (s, 1H, Ph-NH), 8.96 (br, 1H, NHOH), 7.57 (d, *J* = 7.8 Hz, 2H, 2'-H, 6'-H), 7.30 (t, *J* = 7.8 Hz, 2H, 3'-H, 5'-H), 7.05 (t, *J* = 7.3 Hz, 1H, 4'-H), 3.11 (s, 2H, 2-H) ppm. ¹³C NMR (126 MHz, [D₆]DMSO): δ = 165.27 (C-1 or C-3), 163.48 (C-1 or C-3), 138.93 (C-1'), 128.76 (C-3', C-5'), 123.38 (C-4'), 119.07 (C-2', C-6'), 42.03 (C-2) ppm. HRMS (ESI): calcd. for C₉H₉N₂O₃ [M-H]⁻ 193.0619, found: 193.0609. TLC (CH₂Cl₂/MeOH/HCOOH 90:9:1): R_f = 0.15.

Methyl 3-oxo-3-(phenylamino)propanoate (12): Aniline (400 μL, 4.39 mmol) and NEt₃ (1.20 mL, 8.61 mmol) were dissolved in CH₂Cl₂ (10 mL) and cooled to 0 °C. Methyl malonyl chloride (500 μL, 5.24 mmol) was added dropwise over 15 min, and the reaction mixture was stirred at 0 °C for 3 h. The reaction was quenched with cold water (15 mL), and the mixture was diluted with CH₂Cl₂. The organic layer was washed with sat. NaHCO₃ solution (5×40 mL) and dried over Na₂SO₄. The solvent was evaporated under reduced pressure, and the resultant crude product was purified by column chromatography (CH₂Cl₂) to give **12** as a slightly orange solid (523 mg, 62%). ¹H NMR (500 MHz, CDCl₃): δ = 9.15 (br, 1H, NH), 7.55 (d, *J* = 8.1 Hz, 2H, 2'-H, 6'-H), 7.33 (t, *J* = 7.9 Hz, 2H, 3'-H, 5'-H), 7.13 (t, *J* = 7.4 Hz, 1H, 4'-H), 3.80 (s, 3H, OCH₃), 3.49 (s, 2H, 2-H) ppm. ¹³C NMR (126 MHz, CDCl₃): δ = 170.58 (C-1 or C-3), 162.82 (C-1 or C-3), 137.54 (C-1'), 129.15 (C-3', C-5'), 124.76 (C-4'), 120.25 (C-2', C-6'), 52.82 (OCH₃), 41.45 (C-2) ppm. MS (ESI): *m/z* = 216.0 [M+Na]⁺. TLC (petroleum ether/EtOAc 7:3): R_f = 0.10.

Methyl 4-oxo-4-(phenylamino)butanoate (13): Aniline (100 μL, 1.10 mmol) and NEt₃ (300 μL, 2.15 mmol) were dissolved in CH₂Cl₂ (5 mL) and cooled to 0 °C. Methyl succinyl chloride (170 μL, 1.38 mmol) was added dropwise over 10 min, and the reaction mixture was stirred at 0 °C for 3.5 h. The reaction was quenched with cold water (15 mL), and the mixture was diluted with CH₂Cl₂.

The organic layer was washed with sat. NaHCO₃ solution (4 × 30 mL) and dried over Na₂SO₄. The solvent was evaporated under reduced pressure and the resultant crude product was purified by centrifugal TLC (CH₂Cl₂) to give **13** as a white solid (222 mg, 98%). ¹H NMR (500 MHz, CDCl₃): δ = 7.71 (br, 1H, NH), 7.50 (d, *J* = 7.9 Hz, 2H, 2'-H, 6'-H), 7.29 (t, *J* = 7.9 Hz, 2H, 3'-H, 5'-H), 7.09 (t, *J* = 7.4 Hz, 1H, 4'-H), 3.70 (s, 3H, OCH₃), 2.75 (t, *J* = 6.5 Hz, 2H, 2-H or 3-H), 2.66 (t, *J* = 6.5 Hz, 2H, 2-H or 3-H) ppm. ¹³C NMR (126 MHz, CDCl₃): δ = 173.78 (C-1 or C-4), 169.84 (C-1 or C-4), 137.97 (C-1'), 129.07 (C-3', C-5'), 124.35 (C-4'), 119.90 (C-2', C-6'), 52.12 (OCH₃), 32.20 (C-2 or C-3), 29.36 (C-2 or C-3) ppm. HRMS (ESI): calcd. for C₁₁H₁₄NO₃ [*M* + H]⁺ 208.0968, found 208.0961. TLC (petroleum ether/EtOAc 7:3): *R*_f = 0.10.

N-(4-Acetylphenyl)-2-(1H-1,2,3-triazol-1-yl)acetamide (14): Alkyl chloride **21** (60 mg, 0.28 mmol), NEt₃ (90 μL, 0.65 mmol) and 1H-1,2,3-triazole (20 μL, 0.34 mmol) were dissolved in DMF (10 mL) and stirred at RT for 8 d. EtOAc (250 mL) was added, and the organic layer was washed with water (5 × 30 mL) and brine (30 mL) and then dried over Na₂SO₄. The solvent was evaporated under reduced pressure, and the resultant crude product was purified by column chromatography (CH₂Cl₂/MeOH 99:1) to give **14** as a white solid (17 mg, 25%). ¹H NMR (500 MHz, [D₆]DMSO): δ = 10.83 (s, 1H, NH), 8.17 (d, *J* = 0.9 Hz, 1H, 5''-H), 7.96 (d, *J* = 8.8 Hz, 2H, 3'-H, 5'-H), 7.77 (d, *J* = 0.8 Hz, 1H, 4''-H), 7.72 (d, *J* = 8.8 Hz, 2H, 2'-H, 6'-H), 5.41 (s, 2H, 2-H), 2.53 (s, 3H, acetyl-CH₃) ppm. ¹³C NMR (126 MHz, [D₆]DMSO): δ = 196.52 (acetyl-C=O), 164.96 (C-1), 142.69 (C-1'), 133.15 (C-4''), 132.15 (C-4'), 129.61 (C-3', C-5'), 126.55 (C-5''), 118.53 (C-2', C-6'), 52.04 (C-2), 26.45 (acetyl-CH₃) ppm. MS (ESI): *m/z* = 245.0 [*M* + H]⁺. HRMS (ESI): calcd. for C₁₂H₁₃N₄O₂ [*M* + H]⁺ 245.1033, found 245.1030. TLC (CH₂Cl₂/MeOH 95:5): *R*_f = 0.15.

N-(4-Acetylphenyl)-2-(1H-imidazol-1-yl)acetamide (15): General procedure GP1 with 1H-imidazole (41 mg, 0.60 mmol) and alkyl iodide **22** (156 mg, 0.515 mmol) to give **15** as a white solid (47 mg, 38%). ¹H NMR (500 MHz, [D₆]DMSO): δ = 10.65 (s, 1H, NH), 7.95 (d, *J* = 8.8 Hz, 2H, 3'-H, 5'-H), 7.72 (d, *J* = 8.8 Hz, 2H, 2'-H, 6'-H), 7.64 (s, 1H, 2''-H), 7.17 (t, *J* = 1.9 Hz, 1H, 5''-H), 6.90 (t, *J* = 0.9 Hz, 1H, 4''-H), 4.96 (s, 2H, 2-H), 2.53 (s, 3H, acetyl-CH₃) ppm. ¹³C NMR (126 MHz, [D₆]DMSO): δ = 196.50 (acetyl-C=O), 166.43 (C-1), 142.93 (C-1'), 138.35 (C-2''), 131.93 (C-4'), 129.59 (C-3', C-5'), 127.92 (C-4''), 120.76 (C-5''), 118.39 (C-2', C-6'), 49.18 (C-2), 26.43 (acetyl-CH₃) ppm. HRMS (ESI): calcd. for C₁₃H₁₄N₃O₂ [*M* + H]⁺ 244.1081, found 244.1078. TLC (CH₂Cl₂/MeOH 9:1): *R*_f = 0.20.

N-(4-Acetylphenyl)-2-(1H-1,2,4-triazol-1-yl)acetamide (16): General procedure GP1 with 1H-1,2,4-triazol (46 mg, 0.67 mmol) and alkyl iodide **22** (165 mg, 0.545 mmol) to give **16** as a slightly orange solid (87 mg, 65%). ¹H NMR (500 MHz, [D₆]DMSO): δ = 10.76 (s, 1H, NH), 8.56 (s, 1H, 5''-H), 8.01 (s, 1H, 3''-H), 7.95 (d, *J* = 8.8 Hz, 2H, 3'-H, 5'-H), 7.71 (d, *J* = 8.8 Hz, 2H, 2'-H, 6'-H), 5.19 (s, 2H, 2-H), 2.53 (s, 3H, acetyl-CH₃) ppm. ¹³C NMR (126 MHz, [D₆]DMSO): δ = 196.58 (acetyl-C=O), 165.26 (C-1), 151.47 (C-3''), 145.69 (C-5''), 142.73 (C-1'), 132.16 (C-4'), 129.66 (C-3', C-5'), 118.55 (C-2', C-6'), 51.85 (C-2), 26.51 (acetyl-CH₃) ppm. MS (ESI): *m/z* = 245.0 [*M* + H]⁺. HRMS (ESI): calcd. for C₁₂H₁₃N₄O₂ [*M* + H]⁺ 245.1033, found 245.1030. TLC (CH₂Cl₂/MeOH 95:5): *R*_f = 0.10.

N-(4-Acetylphenyl)-2-(1H-tetrazol-1-yl)acetamide (17) and N-(4-acetylphenyl)-2-(2H-tetrazol-2-yl)acetamide (18): General procedure GP1 with 1H-tetrazole (27 mg, 0.39 mmol) and alkyl iodide **22** (101 mg, 0.333 mmol) to give **17** as a white solid (28 mg, 34%) and **18** as a white solid (26 mg, 32%). **17**: ¹H NMR (500 MHz, [D₆]DMSO): δ = 10.90 (s, 1H, NH), 9.43 (s, 1H, 5''-H), 7.96 (d, *J* = 8.8 Hz, 2H, 3'-H, 5'-H), 7.71 (d, *J* = 8.8 Hz, 2H, 2'-H, 6'-H), 5.54 (s, 2H, 2-H), 2.53 (s, 3H, acetyl-CH₃) ppm. ¹³C NMR (126 MHz, [D₆]DMSO): δ = 196.55 (acetyl-C=O), 164.14 (C-1), 145.26 (C-5''), 142.50 (C-1'), 132.27 (C-4'), 129.64 (C-3', C-5'), 118.59 (C-2', C-6'), 50.14 (C-2), 26.46 (acetyl-CH₃) ppm.

MS (ESI): *m/z* = 246.0 [*M* + H]⁺, 268.0 [*M* + Na]⁺. HRMS (ESI): calcd. for C₁₁H₁₃N₅O₂ [*M* + H]⁺ 246.0986, found 246.0982. TLC (CH₂Cl₂/MeOH 95:5): *R*_f = 0.25. **18**: ¹H NMR (500 MHz, [D₆]DMSO): δ = 10.95 (s, 1H, NH), 9.05 (s, 1H, 5''-H), 7.96 (d, *J* = 8.8 Hz, 2H, 3'-H, 5'-H), 7.70 (d, *J* = 8.8 Hz, 2H, 2'-H, 6'-H), 5.78 (s, 2H, 2-H), 2.53 (s, 3H, acetyl-CH₃) ppm. ¹³C NMR (126 MHz, [D₆]DMSO): δ = 196.53 (acetyl-C=O), 163.52 (C-1), 153.42 (C-5''), 142.40 (C-1'), 132.34 (C-4'), 129.61 (C-3', C-5'), 118.65 (C-2', C-6'), 55.05 (C-2), 26.46 (acetyl-CH₃) ppm. HRMS (ESI): calcd. for C₁₁H₁₂N₅O₂ [*M* + H]⁺ 246.0986, found 246.0984. TLC (CH₂Cl₂/MeOH 95:5): *R*_f = 0.40.

N-(4-Acetylphenyl)-2-(2H-tetrazol-5-yl)acetamide (19): A suspension of nitrile **23** (102 mg, 0.505 mmol), NaN₃ (159 mg, 2.45 mmol) and ZnBr₂ (100 mg, 0.444 mmol) in *i*PrOH/water (1:3) was stirred under reflux for 2 d. After cooling to RT, EtOAc (200 mL) was added, and the organic layer was washed with HCl (0.2 M, 3 × 50 mL) and brine (50 mL) and then dried over Na₂SO₄. The solvent was evaporated under reduced pressure, and the resultant crude product was purified by centrifugal TLC (CH₂Cl₂/MeOH 100:0 → 90:10) to give **19** as a white solid (41 mg, 33%). ¹H NMR (500 MHz, [D₆]DMSO): δ = 16.26 (br, 1H, 2''-NH), 10.78 (s, 1H, NH(C=O)), 7.95 (d, *J* = 8.8 Hz, 2H, 3'-H, 5'-H), 7.72 (d, *J* = 8.8 Hz, 2H, 2'-H, 6'-H), 4.20 (s, 2H, 2-H), 2.53 (s, 3H, acetyl-CH₃) ppm. ¹³C NMR (126 MHz, [D₆]DMSO): δ = 196.56 (acetyl-C=O), 165.73 (C-1), 150.82 (C-5''), HMBC, 142.95 (C-1'), 132.11 (C-4'), 129.60 (C-3', C-5'), 118.52 (C-2', C-6'), 31.80 (C-2), 26.48 (acetyl-CH₃) ppm. MS (ESI): *m/z* = 246.0 [*M* + H]⁺. HRMS (ESI): calcd. for C₁₁H₁₂N₅O₂ [*M* + H]⁺ 246.0986, found 246.0980. TLC (CH₂Cl₂/MeOH/HCOOH 94:5:1): *R*_f = 0.50.

N-(4-Acetylphenyl)-2-(1H-imidazol-4-yl)acetamide (20): 2-(1H-imidazol-4-yl)acetic acid hydrochloride (180 mg, 1.11 mmol), HBTU (430 mg, 1.13 mmol) and DIPEA (140 μL, 0.823 mmol) were dissolved in DMF (5 mL). After 5 min stirring at RT, *p*-aminoacetophenone (101 mg, 0.747 mmol) was added, and the reaction mixture was stirred at RT for 27 h. EtOAc (200 mL) was added, and the organic layer was washed with NaHCO₃ solution (1.0 M, 3 × 50 mL) and brine (50 mL) and then dried over Na₂SO₄. The solvent was evaporated under reduced pressure, and the resultant crude product was purified by column chromatography (CH₂Cl₂/MeOH/NEt₃ 90:5:5) to give **20** as a white solid (70 mg, 39%). ¹H NMR (500 MHz, [D₆]DMSO): δ = 11.95 (br, 1H, 1''-NH), 10.44 (s, 1H, NH(C=O)), 7.92 (d, *J* = 8.8 Hz, 2H, 3'-H, 5'-H), 7.73 (d, *J* = 8.8 Hz, 2H, 2'-H, 6'-H), 7.58 (d, *J* = 1.0 Hz, 1H, imidazole-H), 6.94 (s, 1H, imidazole-H), 3.61 (s, 2H, 2-H), 2.52 (s, 3H, acetyl-CH₃) ppm. ¹³C NMR (126 MHz, [D₆]DMSO): δ = 196.46 (acetyl-C=O), 169.29 (C-1), 143.57 (C-1'), 134.95 (imidazole-C), 131.60 (C-4'), 129.47 (C-3', C-5'), 118.25 (C-2', C-6'), 35.87 (C-2), 26.40 (acetyl-CH₃) ppm (due to poor relaxation, two imidazole-carbon nuclei could not be observed, but the respective hydrogen nuclei were found in the ¹H NMR spectrum). HRMS (ESI): calcd. for C₁₃H₁₄N₃O₂ [*M* + H]⁺ 244.1081, found 244.1077. TLC (CH₂Cl₂/MeOH/NEt₃ 85:10:5): *R*_f = 0.25.

N-(4-Acetylphenyl)-2-chloroacetamide (21): *p*-Aminoacetophenone (1.00 g, 7.41 mmol) and DIPEA (1.40 mL, 8.18 mmol) were dissolved in THF (5 mL). Chloroacetyl chloride (650 μL, 8.16 mmol) was added dropwise, and the reaction mixture was stirred at RT for 20 min. The reaction was quenched by addition of MeOH (15 mL). The mixture was then diluted with EtOAc (200 mL), washed with HCl (0.2 M, 3 × 30 mL) and sat. NaHCO₃ solution (3 × 30 mL) and then dried over Na₂SO₄. The solvent was evaporated under reduced pressure to give **21** as a slightly green solid (1.54 g, 98%). ¹H NMR (500 MHz, CDCl₃): δ = 8.41 (s, 1H, NH), 7.98 (d, *J* = 8.7 Hz, 2H, 3'-H, 5'-H), 7.68 (d, *J* = 8.7 Hz, 2H, 2'-H, 6'-H), 4.22 (s, 2H, 2-H), 2.59 (s, 3H, acetyl-CH₃) ppm. ¹³C NMR (126 MHz, CDCl₃): δ = 196.95 (acetyl-C=O), 164.14 (C-1), 141.00 (C-1'), 133.90 (C-4'), 129.89 (C-3', C-5'), 119.39 (C-2', C-6'), 42.99 (C-2), 26.61 (acetyl-CH₃) ppm. HRMS (ESI): calcd. for C₁₀H₁₁ClNO₂ [*M* + H]⁺ 212.0473, found 212.0466. TLC (CH₂Cl₂/MeOH 95:5): *R*_f = 0.55.

N-(4-Acetylphenyl)-2-iodoacetamide (22): Alkyl chloride **21** (364 mg, 1.72 mmol) and KI (859 mg, 5.18 mmol) were dissolved in acetone (20 mL), and the reaction mixture was stirred at RT for 15 h. EtOAc (200 mL) was added, the organic layer was washed with NaHCO₃ solution (0.5 M, 3 × 50 mL), HCl (0.5 M, 3 × 50 mL) and brine (50 mL) and then dried over Na₂SO₄. The solvent was evaporated under reduced pressure to give **22** as a slightly orange solid (472 mg, 91%). ¹H NMR (500 MHz, CDCl₃ + CD₃OD): δ = 7.91 (d, *J* = 9.0 Hz, 2H, 3'-H, 5'-H), 7.63 (d, *J* = 8.8 Hz, 2H, 2'-H, 6'-H), 3.83 (s, 2H, 2-H), 2.55 (s, 3H, acetyl-CH₃) ppm. ¹³C NMR (126 MHz, CDCl₃ + CD₃OD): δ = 197.53 (acetyl-C=O), 166.56 (C-1), 142.42 (C-1'), 133.09 (C-4'), 129.78 (C-3', C-5'), 119.04 (C-2', C-6'), 26.50 (acetyl-CH₃), -0.71 (C-2) ppm. HRMS (ESI): calcd. for C₁₀H₁₁INO₂ [M + H]⁺ 303.9829, found 303.9824. TLC (petroleum ether/EtOAc 7:3): R_f = 0.15.

N-(4-Acetylphenyl)-2-cyanoacetamide (23): Cyanoacetic acid (141 mg, 1.66 mmol), DIPEA (580 μL, 3.33 mmol) and EDC hydrochloride (428 mg, 2.23 mmol) were dissolved in CH₂Cl₂ (10 mL) and the mixture was stirred at RT for 15 min. Then, *p*-aminoacetophenone (205 mg, 1.52 mmol) was added, and the reaction mixture was stirred at RT for 22 h. EtOAc (250 mL) was added, the organic layer was washed with water (2 × 50 mL), HCl (0.2 M, 1 × 50 mL) and brine (50 mL) and then dried over Na₂SO₄. The solvent was evaporated under reduced pressure, and the resultant crude product was purified by column chromatography (CH₂Cl₂/MeOH 98:2) to give **23** as a white solid (176 mg, 57%). ¹H NMR (500 MHz, [D₆]DMSO): δ = 10.62 (s, 1H, NH), 7.95 (d, *J* = 8.8 Hz, 2H, 3'-H, 5'-H), 7.68 (d, *J* = 8.8 Hz, 2H, 2'-H, 6'-H), 3.96 (s, 2H, 2-H), 2.53 (s, 3H, acetyl-CH₃) ppm. ¹³C NMR (126 MHz, [D₆]DMSO): δ = 196.53 (acetyl-C=O), 161.71 (C-1), 142.60 (C-1'), 132.25 (C-4'), 129.58 (C-3', C-5'), 118.52 (C-2', C-6'), 115.69 (CN), 27.01 (C-2), 26.46 (acetyl-CH₃) ppm. HRMS (ESI): calcd. for C₁₁H₁₁N₂O₂ [M + H]⁺ 203.0815, found 203.0813. TLC (CH₂Cl₂/MeOH 95:5): R_f = 0.35.

Sodium 2-((4-acetylphenyl)amino)-2-oxoethane-1-sulfonate (24): To a suspension of alkyl chloride **21** (509 mg, 2.40 mmol) in EtOH (6 mL), a solution of Na₂SO₃ (302 mg, 2.40 mmol) in water (6 mL) was added. The reaction mixture was stirred under reflux for 4 h. The formed precipitate was filtered off, washed with cold water and dried to give **24** as a white solid (473 mg, 70%). ¹H NMR (500 MHz, [D₆]DMSO): δ = 10.31 (s, 1H, NH), 7.92 (d, *J* = 8.8 Hz, 2H, 3'-H, 5'-H), 7.71 (d, *J* = 8.8 Hz, 2H, 2'-H, 6'-H), 3.57 (s, 2H, 1-H), 2.52 (s, 3H, acetyl-CH₃) ppm. ¹³C NMR (126 MHz, [D₆]DMSO): δ = 196.49 (acetyl-C=O), 165.01 (C-2), 143.43 (C-1'), 131.58 (C-4'), 129.47 (C-3', C-5'), 118.18 (C-2', C-6'), 59.10 (C-1), 26.42 (acetyl-CH₃) ppm. HRMS (ESI): calcd. for C₁₀H₁₂NO₅S [M(acid) + H]⁺ 258.0431, found 258.0428. TLC (CH₂Cl₂/MeOH 95:5): R_f = 0.00.

Sodium 2-((4-acetylphenyl)amino)-2-oxoethyl(methyl)phosphinate (25): General procedure GP2 with ethyl ester **27** (50 mg, 0.18 mmol) to give **25** as a white solid (23 mg, 44%). ¹H NMR (500 MHz, [D₆]DMSO): δ = 10.77 (s, 1H, NH), 7.87 (d, *J* = 8.8 Hz, 2H, 3'-H, 5'-H), 7.71 (d, *J* = 8.8 Hz, 2H, 2'-H, 6'-H), 2.96 (d, *J* = 17.7 Hz, 2H, 1-H), 2.50 (br, 3H (under solvent signal), acetyl-CH₃), 1.42 (d, *J* = 14.8 Hz, 3H, PCH₃) ppm. ¹³C NMR (126 MHz, [D₆]DMSO): δ = 196.42 (acetyl-C=O), 166.00 (C-1), 143.69 (C-1'), 131.51 (C-4'), 129.37 (C-3', C-5'), 118.17 (C-2', C-6'), 42.13 (d, *J*_{CP} = 78.7 Hz, C-1), 26.36 (acetyl-CH₃), 16.29 (d, *J*_{CP} = 97.7 Hz, PCH₃) ppm. ³¹P NMR (162 MHz, [D₆]DMSO): δ = 37.80 ppm. HRMS (ESI): calcd. for C₁₁H₁₃NO₄P [M(acid) + H]⁺ 256.0733, found: 256.0730. TLC (CH₂Cl₂/MeOH/HCOOH 85:13:2): R_f = 0.05.

Disodium 2-((4-acetylphenyl)amino)-2-oxoethyl)phosphonate (26): General procedure GP2 with ethyl ester **28** (182 mg, 0.581 mmol) to give **26** as a slightly orange solid (89 mg, 60%). ¹H NMR (500 MHz, CD₃OD): δ = 8.62 (d, *J* = 8.8 Hz, 3'-H, 5'-H), 8.27 (d, *J* = 8.8 Hz, 2'-H, 6'-H), 3.64 (d, *J* = 21.0 Hz, 1-H), 3.26 (s, 3H, acetyl-

CH₃) ppm. ¹³C NMR (126 MHz, CD₃OD): δ = 213.57 (acetyl-C=O), 179.12 (C-2), 153.54 (C-1'), 143.67 (C-4'), 141.13 (C-3', C-5'), 131.27 (C-2', C-6'), 49.60 (d, *J*_{CP} = 122.2 Hz, C-1), 37.16 (acetyl-CH₃). ³¹P NMR (203 MHz, CD₃OD): δ = 15.82 ppm. HRMS (ESI): calcd. for C₁₃H₂₁NO₄P [M(acid) + H]⁺ 258.0526, found: 258.0523.

Ethyl 2-((4-acetylphenyl)amino)-2-oxoethyl(methyl)phosphinate (27): Alkyl chloride **21** (113 mg, 0.536 mmol) was dissolved in a mixture of toluene (2 mL) and THF (2 mL). At 100 °C, diethyl methylphosphonate (200 μL, 1.33 mmol) was added dropwise over 10 min. The reaction mixture was stirred at 100 °C for 23 h. After cooling to RT, the solvent was evaporated under reduced pressure, and the resultant crude product was purified by column chromatography (CH₂Cl₂/MeOH 98:2) to give **27** as a white solid (113 mg, 75%). ¹H NMR (500 MHz, CDCl₃): δ = 9.97 (s, 1H, NH), 7.73 (d, *J* = 8.8 Hz, 2H, 3'-H, 5'-H), 7.51 (d, *J* = 8.8 Hz, 2H, 2'-H, 6'-H), 4.19–4.12 (m, 2H, ethyl-1-H), 3.19 (dd, *J* = 18.9, 14.3 Hz, 1H, 1-H_a), 2.99 (dd, *J* = 14.3, 14.3 Hz, 1H, 1-H_b), 2.50 (s, 3H, acetyl-CH₃), 1.72 (d, *J* = 14.5 Hz, 3H, PCH₃), 1.37 (t, *J* = 7.0 Hz, 3H, ethyl-2-H) ppm. ¹³C NMR (126 MHz, CDCl₃): δ = 197.02 (acetyl-C=O), 163.42 (d, *J*_{CP} = 3.8 Hz, C-2), 142.54 (C-1'), 132.74 (C-4'), 129.52 (C-3', C-5'), 118.86 (C-2', C-6'), 61.57 (d, *J*_{CP} = 6.5 Hz, ethyl-C-1), 40.35 (d, *J*_{CP} = 81.2 Hz, C-1), 26.48 (acetyl-CH₃), 16.71 (d, *J*_{CP} = 6.2 Hz, ethyl-C-2), 14.78 (d, *J*_{CP} = 97.3 Hz, PCH₃) ppm. ³¹P NMR (203 MHz, CDCl₃): δ = 49.31 ppm. HRMS (ESI): calcd. for C₁₃H₁₈NO₄P [M + H]⁺ 284.1046, found 284.1043. TLC (CH₂Cl₂/MeOH 95:5): R_f = 0.15.

Diethyl 2-((4-acetylphenyl)amino)-2-oxoethyl)phosphonate (28): Alkyl chloride **21** (146 mg, 0.692 mmol) was suspended in triethylphosphite (2.30 mL, 13.3 mmol) and the reaction mixture was stirred under reflux for 18 h. After cooling to RT, the solvent was evaporated under reduced pressure, and the resultant oily crude product was purified by column chromatography (petroleum ether/EtOAc 1:2 → 1:5) to give **28** as a white solid (193 mg, 89%). ¹H NMR (500 MHz, CDCl₃): δ = 9.53 (s, 1H, NH), 7.81 (d, *J* = 8.7 Hz, 2H, 3'-H, 5'-H), 7.56 (d, *J* = 8.8 Hz, 2H, 2'-H, 6'-H), 4.24–4.18 (m, 4H, ethyl-1-H), 3.08 (d, *J* = 21.1 Hz, 2H, 1-H), 2.53 (s, 3H, acetyl-CH₃), 1.38 (t, *J* = 7.1 Hz, 6H, ethyl-2-H) ppm. ¹³C NMR (126 MHz, CDCl₃): δ = 197.03 (acetyl-C=O), 162.61 (d, *J* = 3.9 Hz, C-2), 142.32 (C-1'), 132.94 (C-4'), 129.65 (C-3', C-5'), 118.98 (C-2', C-6'), 63.33 (d, *J*_{CP} = 6.8 Hz, ethyl-C-1), 36.50 (d, *J*_{CP} = 129.3 Hz, C-1), 26.51 (acetyl-CH₃), 16.49 (d, *J*_{CP} = 6.1 Hz, ethyl-C-2) ppm. ³¹P NMR (203 MHz, CDCl₃): δ = 22.49 ppm. MS (ESI): *m/z* = 336.0 [M + Na]⁺. TLC (CH₂Cl₂/MeOH 9:1): R_f = 0.55.

FRET-based collagenase inhibition assay: The peptidase domain (PD) of ColH (Uniprot: Q46085; Leu331-Gly721) and the collagenase unit of ColQ1 (ColQ1-CU; Uniprot: B9 J354; Tyr94-Gly765) were expressed and purified as previously described.^[24] IC₅₀ measurements were performed as previously reported.^[13] ColH-PD was pretreated with the compounds at RT for 1 h. The reaction was initiated by the addition of 2 μM of the peptide substrate Mca-Ala-Gly-Pro-Gly-Pro-Dpa-Gly-Arg-NH₂ (FS1-1; Mca = (7-methoxycoumarin-4-yl)acetyl; Dpa = *N*-3-(2,4-dinitrophenyl)-L-2,3-diaminopropionyl). The increase in fluorescence was monitored for 2 min (λ_{ex} = 328 nm; λ_{em} = 392 nm) at 25 °C. The final concentrations were 10 nM ColH-PD and 1 nM ColQ1-CU, respectively, 2 μM FS1-1, 250 mM HEPES pH 7.5, 400 mM NaCl, 10 mM CaCl₂, 10 μM ZnCl₂, 2% DMSO and eight different compound concentrations. The percentage of enzyme inhibition was calculated in relation to a blank reference without compound added. All experiments were performed in triplicates and repeated at least three times. IC₅₀ values were determined using nonlinear regression with a constant Hill slope of -1. Regression analysis was performed using GraphPad Prism 5 (Graph Pad Software, San Diego, CA, USA).

MMP inhibition assay: The catalytic domains of MMP-1, -2, -3, -7, -8, and -14 along with the Sensolyte 520 generic MMP activity kit were purchased from AnaSpec (Fremont, CA, USA). The

assay was performed as previously described using Batimastat as a positive control^[13,25] and according to the guidelines of the manufacturer.

HDAC inhibition assay: HDAC3 and HDAC8 inhibitor screening kits were purchased from Sigma–Aldrich. The assay was performed according to the guidelines of the manufacturer. Fluorescence signals were measured in a CLARIOstar plate reader (BMG Labtech).

TACE inhibition assay: A TACE (ADAM-17) inhibitor screening assay kit was purchased from Sigma–Aldrich. The assay was performed according to the guidelines of the manufacturer. Fluorescence signals were measured in a CLARIOstar plate reader (BMG Labtech).

Cytotoxicity assay: HepG2, HEK293, or A549 cells (2×10^5 cells per well) were seeded in 24-well, flat-bottomed plates. Culturing of cells, incubations, and OD measurements were performed as previously described^[26] with minor modifications. 24 h after seeding the cells, the incubation was started by the addition of compounds at a final DMSO concentration of 1%. The living cell mass was determined after 48 h. At least two independent measurements were performed for each compound.

Zebrafish embryo toxicity assay: Toxicity testing was performed according to the procedure described in the literature^[27] with minor modifications using zebrafish embryos of the AB wild-type line at 1 d post fertilisation (dpf) as previously reported.^[16] All of the described experiments were performed with zebrafish embryos <120 h post-fertilisation (hpf) and are not classified as animal experiments according to EU Directive 2010/63/EU. Protocols for husbandry and care of adult animals were in accordance with the German Animal Welfare Act (§11 Abs. 1 TierSchG).

Ex vivo pig skin degradation assay: The assay was performed as previously reported^[16] using explants from pig ears in a 24-well plate. Compound **26** was preincubated with 300 nM of ColQ1, 4 mM CaCl₂, 10 μM ZnCl₂ in DMEM medium at 37 °C and 5% CO₂ for 1 h. After preincubation, one skin explant was added into each well and incubated at 37 °C and 5% CO₂ for 24 h under 300 rpm shaking. Hydroxyproline release was measured using a hydroxyproline assay kit (Sigma–Aldrich) according to the guidelines of the manufacturer. Absorbance was measured using a PHERAstar plate reader (BMG Labtech). The absorbance values were converted into hydroxyproline concentrations (μg/mL) using a calibration curve of hydroxyproline (Figures S1 and S2 in the Supporting Information). The absolute concentrations were converted into percentages by setting the concentration of the 0 μM value to 100% and calculating all values from each experiment separately.

Acknowledgements

We thank Dr. Stefan Boettcher and Stefanie Weck for the measurements of high-resolution mass spectra as well as Nathalie Andreia, Martina Jankowski, Jeannine Jung, Dennis Jener and Martina Wiesbauer for technical support. We acknowledge financial support by the Austrian Science Fund (FWF, grants P 31843 (E.S.) and W 01213 (H.B.)), the Austrian Federal Ministry of Science, Research, and Economy (H.B.), the European Research Council (ERC starting grant 757913, A.K.H.H.), and by the Helmholtz Association's Initiative and Networking Fund (A.K.H.H.). Open access funding enabled and organized by Projekt DEAL.

Conflict of Interest

The authors declare no conflict of interest.

Keywords: anti-infectives · drug design · medicinal chemistry · metalloenzymes · structure–activity relationships

- [1] a) J. O'Neill, *Antimicrobial Resistance: Tackling a Crisis for the Health and Wealth of Nations*, UK Government & Wellcome Trust, London, **2014**; b) *Drug-Resistant Infections: A Threat to Our Economic Future*, The World Bank, Washington DC, **2017**.
- [2] *No Time to Wait: Securing the Future from Drug-Resistant Infections*, The World Health Organization, **2019**.
- [3] a) A. E. Clatworthy, E. Pierson, D. T. Hung, *Nat. Chem. Biol.* **2007**, *3*, 541–548; b) D. A. Rasko, V. Sperandio, *Nat. Rev. Drug Discovery* **2010**, *9*, 117–128; c) M. B. Calvert, V. R. Jumde, A. Titz, *Beilstein J. Org. Chem.* **2018**, *14*, 2607–2617.
- [4] a) C. L. Hatheway, *Clin. Microbiol. Rev.* **1990**, *3*, 66–98; b) C. T. Supuran, in *Drug Design of Zinc-Enzyme Inhibitors* (Eds.: C. T. Supuran, J.-Y. Winum), Wiley, Hoboken, **2009**, pp. 721–729.
- [5] a) H. Bruggemann, S. Baumer, W. F. Fricke, A. Wiezer, H. Liesegang, I. Decker, C. Herzberg, R. Martinez-Arias, R. Merkl, A. Henne, G. Gottschalk, *Proc. Natl. Acad. Sci. USA* **2003**, *100*, 1316–1321; b) M. P. Burke, K. Opeskin, *Am. J. Forensic Med. Pathol.* **1999**, *20*, 158–162.
- [6] a) R. Stone, *Science* **2002**, *297*, 1110–1112; b) S. S. Arnon, R. Schlechter, T. V. Inglesby, D. A. Henderson, J. G. Bartlett, M. S. Ascher, E. Eitzen, A. D. Fine, J. Hauer, M. Layton, S. Lillibridge, M. T. Osterholm, T. O'Toole, G. Parker, T. M. Perl, P. K. Russell, D. L. Swerdlow, K. Tonat, *J. Am. Med. Assoc.* **2001**, *285*, 1059–1070.
- [7] D. J. Harrington, *Infect. Immun.* **1996**, *64*, 1885–1891.
- [8] a) U. Eckhard, P. F. Huesgen, H. Brandstetter, C. M. Overall, *J. Proteomics* **2014**, *100*, 102–114; b) M. R. Popoff, P. Bouvet, *Future Microbiol.* **2009**, *4*, 1021–1064.
- [9] a) N. Oshima, Y. Narukawa, T. Takeda, F. Kiuchi, *J. Nat. Med.* **2013**, *67*, 240–245; b) A. Scozzafava, C. T. Supuran, *Bioorg. Med. Chem. Lett.* **2002**, *12*, 2667–2672; c) M. Ilies, M. D. Banciu, A. Scozzafava, M. A. Ilies, M. T. Capriou, C. T. Supuran, *Bioorg. Med. Chem.* **2003**, *11*, 2227–2239; d) B. W. Clare, A. Scozzafava, C. T. Supuran, *J. Med. Chem.* **2001**, *44*, 2253–2258; e) C. T. Supuran, A. Scozzafava, *Eur. J. Pharm. Sci.* **2000**, *10*, 67–76; f) M. Amélia Santos, S. Marques, M. Gil, M. Tegoni, A. Scozzafava, C. T. Supuran, *J. Enzyme Inhib. Med. Chem.* **2003**, *18*, 233–242.
- [10] a) M. D. Shoulders, R. T. Raines, *Ann. Rev. Biochem.* **2009**, *78*, 929–958; b) M. Gauza-Włodarczyk, L. Kubisz, D. Włodarczyk, *Int. J. Biol. Macromol.* **2017**, *104*, 987–991.
- [11] U. Eckhard, E. Schönauer, D. Nüss, H. Brandstetter, *Nat. Struct. Mol. Biol.* **2011**, *18*, 1109–1114.
- [12] a) B. W. Matthews, *Acc. Chem. Res.* **1988**, *21*, 333–340; b) B. L. Vallee, D. S. Auld, *Proc. Natl. Acad. Sci. USA* **1990**, *87*, 220–224; c) L. L. Johnson, A. G. Pavlovsky, A. R. Johnson, J. A. Janowicz, C. F. Man, D. F. Ortwine, C. F. Purchase II, A. D. White, D. J. Hupe, *J. Biol. Chem.* **2000**, *275*, 11026–11033; d) D. Xu, H. Guo, *J. Am. Chem. Soc.* **2009**, *131*, 9780–9788.
- [13] E. Schönauer, A. M. Kany, J. Hauptenthal, K. Hüsecken, I. J. Hoppe, K. Voos, S. Yahiaoui, B. Elsässer, C. Ducho, H. Brandstetter, R. W. Hartmann, *J. Am. Chem. Soc.* **2017**, *139*, 12696–12703.
- [14] a) H. Nagase, R. Visse, G. Murphy, *Cardiovasc. Res.* **2006**, *69*, 562–573; b) G. B. Fields, *J. Biol. Chem.* **2013**, *288*, 8785–8793.
- [15] a) F. Graef, B. Vukosavljevic, J.-P. Michel, M. Wirth, O. Ries, C. De Rossi, M. Windbergs, V. Rosilio, C. Ducho, S. Gordon, C.-M. Lehr, *J. Controlled Release* **2016**, *243*, 214–224; b) H. Nikaido, *Science* **1994**, *264*, 382–388.
- [16] J. Konstantinović, S. Yahiaoui, A. Alhayek, J. Hauptenthal, E. Schönauer, A. Andreas, A. M. Kany, R. Müller, J. Köhnke, F. Berger, M. Bischoff, R. W. Hartmann, H. Brandstetter, A. K. H. Hirsch, *J. Med. Chem.* **2020**, *63*, 8359–8368.
- [17] a) R. A. Cuperus, A. O. Muijsers, R. Wever, *Arthritis Rheumatism* **1985**, *28*, 1228–1233; b) F.-M. Klingler, T. A. Wichelhaus, D. Frank, J. Cuesta-Bernal, J. El-Delik, H. F. Müller, H. Sjuts, S. Göttig, A. Koenigs, K. M. Pos, D. Pogoryelov, E. Proschak, *J. Med. Chem.* **2015**, *58*, 3626–3630; c) R. M. Rydzewski, *Real World Drug Discovery: A Chemist's Guide to Biotech and Pharmaceutical Research*, Elsevier, Oxford, **2008**.
- [18] a) J. A. Jacobsen, J. L. Major Jourden, M. T. Miller, S. M. Cohen, *Biochim. Biophys. Acta Mol. Cell Res.* **2010**, *1803*, 72–94; b) C. Temperini, A.

- Innocenti, A. Guerri, A. Scozzafava, S. Rusconi, C. T. Supuran, *Bioorg. Med. Chem. Lett.* **2007**, *17*, 2210–2215; c) B. Trzaskowski, L. Adamowicz, P. A. Deymier, *J. Biol. Inorg. Chem.* **2007**, *13*, 133–137; d) L. Birch, R. Bachofen, *Experientia* **1990**, *46*, 827–834; e) J. R. Van Wazer, C. F. Callis, *Chem. Rev.* **1958**, *58*, 1011–1046.
- [19] a) R. A. Black, C. T. Rauch, C. J. Kozlosky, J. J. Peschon, J. L. Slack, M. F. Wolfson, B. J. Castner, K. L. Stocking, P. Reddy, S. Srinivasan, N. Nelson, N. Boiani, K. A. Schooley, M. Gerhart, R. Davis, J. N. Fitzner, R. S. Johnson, R. J. Paxton, C. J. March, D. P. Cerretti, *Nature* **1997**, *385*, 729–733; b) M. L. Moss, S.-L. C. Jin, M. E. Milla, W. Burkhart, H. L. Carter, W.-J. Chen, W. C. Clay, J. R. Didsbury, D. Hassler, C. R. Hoffman, T. A. Kost, M. H. Lambert, M. A. Leesnitzer, P. McCauley, G. McGeehan, J. Mitchell, M. Moyer, G. Pahel, W. Rocque, L. K. Overton, F. Schoenen, T. Seaton, J.-L. Su, J. Warner, D. Willard, J. D. Becherer, *Nature* **1997**, *385*, 733–736.
- [20] D. Schlüter, M. Deckert, *Microb. Infect.* **2000**, *2*, 1285–1292.
- [21] P. Sensi, *Clin. Infect. Dis.* **1983**, *5*, S402–S406.
- [22] a) G. Minotti, P. Menna, E. Salvatorelli, G. Cairo, L. Gianni, *Pharmacol. Rev.* **2004**, *56*, 185–229; b) C. Bertazzoli, C. Rovero, L. Ballerini, B. Lux, F. Balconi, V. Antongiovanni, U. Magrini, *Toxicol. Appl. Pharmacol.* **1985**, *79*, 412–422.
- [23] a) A. L. Rubinstein, *Expert Opin. Drug Metab. Toxicol.* **2006**, *2*, 231–240; b) Y. Li, X. Miao, T. Chen, X. Yi, R. Wang, H. Zhao, S. M.-Y. Lee, X. Wang, Y. Zheng, *Colloids Surf. B* **2017**, *156*, 227–235; c) U. J. Pyati, A. T. Look, M. Hammerschmidt, *Sem. Cancer Biol.* **2007**, *17*, 154–165; d) P. McGrath, C.-Q. Li, *Drug Discovery Today* **2008**, *13*, 394–401.
- [24] a) U. Eckhard, E. Schönauer, H. Brandstetter, *J. Biol. Chem.* **2013**, *288*, 20184–20194; b) I. J. Hoppe, H. Brandstetter, E. Schönauer, *Sci. Rep.* **2021**, *11*, 4187.
- [25] A. M. Kany, A. Sikandar, J. Hauptenthal, S. Yahiaoui, C. K. Maurer, E. Proschak, J. Köhnke, R. W. Hartmann, *ACS Infect. Dis.* **2018**, *4*, 988–997.
- [26] J. Hauptenthal, C. Baehr, S. Zeuzem, A. Piiper, *Int. J. Cancer* **2007**, *121*, 206–210.
- [27] J. Maes, L. Verlooy, O. E. Buenafe, P. A. M. de Witte, C. V. Esguerra, A. D. Crawford, *PLoS One* **2012**, *7*, e43850.

Manuscript received: December 23, 2020

Accepted manuscript online: January 27, 2021

Version of record online: March 16, 2021